Title

The role of basicity in selective C-H bond activation by transition metal-oxidos.

Journal

Dalton Transactions: an international journal of inorganic chemistry, 52(32)

Authors

Borovik, Andrew
Follmer, Alec

Publication Date

2023-08-15

DOI

10.1039/d3dt01781h

Peer reviewed

Published in final edited form as:
Dalton Trans. ; 52(32): 11005–11016. doi:10.1039/d3dt01781h.

The Role of Basicity in Selective C–H Bond Activation by Transition Metal-Oxidos

Alec H. Follmer[*], **A. S. Borovik**[*]
Department of Chemistry, University of California–Irvine, Irvine, CA 92697-3900

Abstract

The development of (bio)catalysts capable of selectively activating strong C–H bonds is a continuing challenge in modern chemistry. In both metalloenzymes and synthetic systems capable of activating C–H bonds, transition metal-oxido intermediates serve as the active species for reactivity whose thermodynamic properties influence the bond strengths they are capable of activating. In this Frontier article, we present current ideas of how the basicity of transition metal-oxidos impacts their reactivity with C–H bonds and present new opportunities within this field. We highlight recent insights into the role basicity plays in the activation process and its influence on mechanism, as well as the important role that secondary coordination sphere effects, such as hydrogen bonds, in tuning the basicity of the metal-oxido species is discussed.

Graphical Abstract

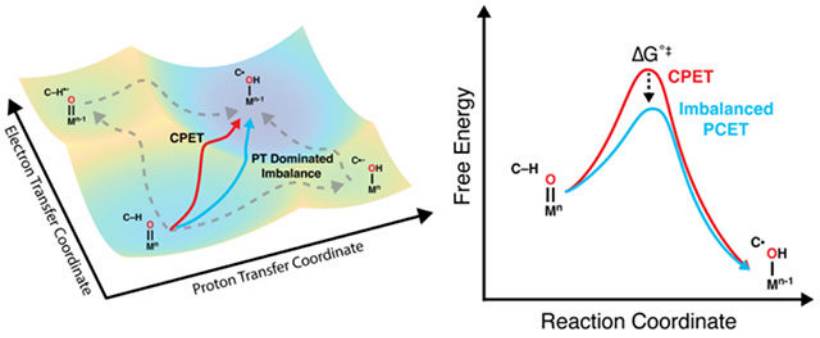

Introduction

The selective functionalization of C–H bonds is a fundamental challenge in modern chemistry. Both the thermodynamic stability and ubiquity of C–H bonds makes the design of catalysts capable of their selective activation difficult because the juxtaposition of potency and selectivity in catalysis, in which an increase in reactivity often results in loss of selectivity.[1,2] In biology, metalloenzymes utilize a combination of transition metallocofactors and elements of their macromolecular structures to circumvent this

[*]Corresponding Authors: afollmer@uci.edu, aborovik@uci.edu.

Conflicts of interest
There are no conflicts to declare.

tradeoff.[3,4] This control is exemplified by transition metallocofactors that achieve high-valent oxidation states, as they are potent catalysts that could lead to nonspecific reactivity leading to afford harmful and undesirable products. To maintain selectivity, metalloenzymes have evolved several strategies to control both the formation of these high-valent states as well as the orientation of substrates within their active sites. Through electrostatic interactions, non-polar contacts, and hydrogen bonds (H-bonds), substrates are positioned within active sites whereby the substrate sites to be reacted upon are nearest the catalytic center. This combination of structure, dynamics, and function remains unrivaled by synthetic systems.

A class of metalloenzymes that utilize these concepts are those that cleave C–H bonds through the use of an Fe-containing cofactor and dioxygen as the primary oxidant.[2,5–7] The binding and activation of O_2 by Fe cofactors results in the formation of transient monomeric Fe^{IV}–oxido intermediates which serve as the catalytically competent species for C–H bond functionalization. The mechanisms that explain the reactivity of these intermediates and the factors that control their function are still the subject of continued investigation. In this Frontier, we present the current understanding of C–H bond activation by metal-oxidos in both metalloenzymes and synthetic systems and provide our perspective on opportunities for developments in the field. We emphasize recent insights into the role that basicity of transition metal-oxidos has in the activation process, its impact on mechanism, and how secondary coordination sphere effects, like H-bonds, can have a significant influence on function.

Thermodynamic Considerations

One way to gauge whether a C–H bond may be activated is by evaluating its bond strength, commonly reported in terms of either its bond dissociation enthalpy (BDE) or bond dissociation free energy (BDFE). In nature, C–H bond functionalization is initiated through the homolytic cleavage of the C–H by a high-valent metal-oxido intermediate, which forms a carbon containing radical and a metal-hydroxido species – note that this new hydroxide species is reduced by one electron from the metal–oxido species (Figure 1A).[6,7] From a ground state thermodynamic perspective, for a reaction to be spontaneous, the resultant O–H bond must be at least as strong as the bond that was broken; thus, the BDFE of the metal-hydroxido O–H bond formed in the reaction acts as the key determinant for the C–H bonds that a particular metalloenzyme can activate. The considerations that govern the BDFE of the resultant O–H bond are described by the Bordwell equation (eq 1) consisting of the appropriate $E_{1/2}$ and related pK_a value for the conjugate acid (M-OH), and a solvent dependent term C_g (Figure 1B).[8–12]

$$\begin{aligned}\mathrm{BDFE_{O-H}\ (kcal\ mol^{-1})} = 23.06\ \mathrm{(kcal\ mol^{-1}\ V^{-1})}\ E_{1/2}\mathrm{(V)} + 1.37\ \mathrm{(kcal\ mol^{-1})}\\ pK_a + \mathrm{C_g\ (kcal\ mol^{-1})}\end{aligned} \quad (1)$$

Eq 1 illustrates that the process of homolytic C–H bond activation is formally equivalent to that of abstracting a hydrogen atom with the net transfer of a proton and electron. This formal hydrogen atom transfer (HAT) is a subdomain within the larger field of proton-

coupled electron transfer (PCET), where the mechanisms of transfer and localization of the proton and electron act as the classifying criteria. Our goal here is to demonstrate how PCET concepts can be applied to mechanisms of C–H bond cleavage by biological and synthetic transition metal-oxido complexes. PCET is a broad fundamental process and has been reviewed in several comprehensive accounts.[11–17] The type of PCET we are concerned with is a variation where the electron and proton derive from the same place but end-up in different locations whereby the proton transfers to the oxido ligand and the electron is transferred to the metal center (Figure 1A).

Within this class of reactions, there are several possible mechanisms of PCET and the three limiting cases are commonly represented by a square-scheme (Figure 1B) with the "uncoupled" paths or stepwise proton transfer-electron transfer (PT–ET) and stepwise electron transfer-proton transfer (ET–PT) defining the outer edges and a concerted proton-electron transfer (CPET) represented by the diagonal. However, a growing area of interest in inorganic chemistry are mechanisms of C–H bond activation that fall between these limits off the diagonal often referred to as "asynchronous", "nonsynchronous", or "imbalanced" PCET.[18–30] These types of reactions are still considered concerted, as compared to stepwise, because a thermodynamically stable intermediate is not formed during the transfer process but differ from CPET as the degree of charge transfer or delocalization of either the proton or electron lags behind the other (Figure 2). Nonsynchronous transfer, imbalanced transition states, and nonadiabatic PCET have a rich history in physical organic chemistry where there are numerous examples of these concepts.[31–33] In fact, anytime a reaction involves more than one process such as making or breaking bonds, changes in charge localization, or solvation, it has the possibility to pass through an imbalanced transition state making the potential for asynchronous mechanisms more likely than CPET.[31] With this said, it is then perhaps surprising that most studies of C–H bond activation by transition metal-oxidos involving synthetic Fe^{IV}=O systems appear to follow the CPET path.[34–41] Experimentally, this is verified by a linear relationship between the log of the second order rate constant ($\log(k)$) and the BDFE of the C–H bond. This result follows from the Bell–Evans–Polanyi (BEP) principle,[42,43] which predicts that either a decrease in $BDFE_{C–H}$ of the cleaved C–H bond or an increase in $BDFE_{O–H}$ of the M–OH bond formed leads to an exponential increase in observed rate constant (Figure 2A,B). As a result of this correlation, deviations from this relationship provide indications that the contributions of the energetics of the PT and ET processes to the overall activity are not equal. When situations like this arise, it hints either at the presence of an imbalance in the transition state and/or nonadiabatic contributions to the rate constant. In some cases, mechanistic insight can be found in examining the individual variables that control the $BDFE_{O–H}$ such as its pK_a and the $E_{1/2}$ of its associated conjugate acid. Plotting these factors that determine bond strength versus $\log(k)$ have proved valuable in determination of PCET mechanisms exhibiting imbalanced transition states.[22,23,27,30]

While discussions of semiclassical CPET provide important insight into the mechanisms of C–H bond activation, essential aspects of this reaction cannot be sufficiently explained without a more complete quantum mechanical treatment. Effects like nonadiabatic couplings and tunneling can alter the mechanisms and therefore rates of both the proton and electron

transfer.[14,25,32] The necessity of including these effects depends on the nature of the mechanism or identity of the transition state (i.e., whether it is concerted or imbalanced) because the degree of nonadiabaticity and tunneling will directly depend on the proximity of the two potential energy surfaces near their crossing point. The closer the passage through the transition state is to a conical intersection, the more nonadiabatic it becomes. The role of nonadiabatic couplings in PCET and C–H bond activation specifically have been extensively theoretically treated.[13,14,25–27,32] However, unambiguous delineation of these mechanisms experimentally is challenging as they are controlled by factors that are hard to isolate and systematically control such as the symmetry and energy differences between the ground and excited states of the reactants and products.

Controlling Basicity for Selectivity in C–H bond Activation

Although quantum mechanical effects play a significant role in describing C–H bond activation, as experimental chemists, we are focused on controllable aspects like the identities and concentrations of the reactants and metal complexes, as well as environmental factors like solvent composition, temperature, and pressure. Together these reaction conditions govern the likelihood of all possible mechanisms our compounds can take. As such, we want to understand the aspects of coordination complexes and metalloenzyme active sites that increase the likelihood for selective activation of strong C–H bonds and which predispose them towards transition states and mechanisms that improve their reactivity based solely on ground state thermodynamic properties of our reactants and products. As previously mentioned, from a thermodynamic perspective, one strategy to achieve the functionalization of stronger C–H bonds is to increase the strength of the formed O–H bond; from eq 1, there are two parameters that can be modulated to change its strength: acidity and redox potential. Modulation of the redox potential presents a chemically logical strategy, but often comes at a loss of stability and selectivity. Tuning of the pK_a, on the other hand, is a relatively unexplored yet appealing approach for achieving selective C–H bond activation.[23,27,44–48] Not only does a more basic metal-oxido decrease the oxidation potential required for a given C–H bond, but also can be used to select for the most acidic C–H bond rather than one with the weakest BDFE. Modulation of the redox potential and pK_a are not entirely independent, however there are several strategies that can be employed to achieve greater alteration of one over the other. Looking to nature, we find examples of this type of selective modification of these factors where achieving the activation of strong bonds is necessary, but the regulation of redox potentials is crucial to preventing unwanted side reactions or damage to the protein scaffold.

Protein Examples

Cytochromes P450 (P450s) are the canonical examples of C–H bond activation catalysts in biological systems.[6,49] They play essential roles in metabolism as well as the biosynthesis of many natural products. P450s are a superfamily of monooxygenases that utilize molecular dioxygen and their heme cofactors to activate strong C–H bonds of their substrates (with BDFEs from ~60-100 kcal/mol). Although there are many heme enzymes, only P450s are capable of functionalizing alkane C–H bonds. This increased reactivity is attributed to P450s having an axial cysteine ligation to their heme cofactor rather than a histidine commonly

found in other heme enzymes.[45] During the catalytic cycle, dioxygen binds to a heme Fe^{II} species and is cleaved via a series of ET and PT steps to form the active intermediate, an Fe^{IV}=O porphyrin radical (compound I).[6,50,51] Although compound I is formed in the catalytic cycles of many heme-enzymes, it was proposed that the increased electron donation from the axial thiolate ligand weakens the Fe^{IV}=O bond and raises the basicity of the oxido ligand, resulting in the ability of P450s to activate stronger C–H bonds.[49,52–55] Support for this premise comes for the experimentally determined pK_a value of 12 for compound II, the ferryl hydroxide species formed after C–H bond cleavage. This value is unusually high for metal-oxido complexes, including other Fe heme proteins, that are normally less than 5.[45,56]

The pK_a values of metal-oxidos is mainly determined by the ligands within the primary coordination sphere, but secondary coordination sphere interactions such as H-bonds are also thought to regulate the basicity, leading to differences in reactivity between metalloenzymes bearing identical cofactors. For example, the heme cofactor of chloroperoxidase (CPO) is also attached to its protein host via cysteine ligation; however, it is unable to match the reactivity of P450s toward C–H bonds. One proposed explanation for this discrepancy in reactivity is the differences in the H-bonding networks to their respective thiolate ligands (Figure 3). CPO exhibits stronger H-bonds to its thiolate ligand than what is found in P450s, resulting in a longer Fe–S bond by 0.1 Å.[57] The different potency of the two proteins has thus been attributed to their dissimilar Fe–S bond lengths. Any variation in the Fe–S bond length will lead to differences in both the electron donating ability of the S-atom to the trans oxido ligand as well as the unpaired spin population distribution and covalency within the Fe=O unit.

Within a broader context, the role of unpaired spin-density on the oxido ligand, and spin-states generally, have been proposed as being key determinants for facile C–H bond activation;[58–61] however, other argue spin-based effects have a limited role in dictating reactivity.[62] Direct experimental observation and correlation of the degree of spin density with reactivity is challenging and, accordingly these arguments have largely been driven by theory. One recent exception is the work of Field and Green, who utilized electron nuclear double resonance (ENDOR) spectroscopy to explore these differences and measured the electron spin and charge density on the oxido ligands of three compound I type intermediates of chloroperoxidase (CPO), a P450 and a P450 with a selenium substituted axial ligation (SeP450).[55] The utility of this approach was first exemplified by Hoffman and coworkers to assign the identity and spin distributions of compound I species horseradish (HRP) and cytochrome c (CCP) peroxidases and CPO, respectively. In their work, Field and Green prepared ^{17}O-labelled compound I species of CPO, P450 and SeP450 and experimentally examined the resultant ^{17}O hyperfine coupling to directly measure the spin populations on the oxido ligands. The terminal oxido ligand of compound I in P450 exhibited 20% less spin population that that in compound I of CPO. Hence, despite having a longer Fe–S bond and a less donating axial ligand, CPO exhibited increased unpaired electron spin density on the oxido ligand compared to the P450 systems. This insight is crucial because the difference in reactivity between these two systems is controlled by non-covalent interactions to the S-ligand trans to the oxido. Theoretical support for the increased charge donation comes from a simple Hückel-type molecular orbital (MO) analysis that

suggested an inverse relationship between electron donation and oxygen spin population. The central point of this argument is that stronger electron donation of the axial ligand decreases the unpaired spin population on oxido ligand because increased donation raises the energy of the d-orbitals relative to the O p-orbitals. Constrained density functional theory (CDFT) calculations further supported this conclusion whereby it was demonstrated that as negative charge accumulates on the oxido ligand, the associated spin density decreases.

Comparison of CPO and P450 to the selenium substituted P450 yielded some surprising results. The isoelectronic substitution of axially donors from Se to S resulted in a more reactive and less stable compound I species in SeP450 compared to the native system. Based on the inverse correlation found between spin density and charge density in CPO and P450, one would expect the oxygen spin-density of SeCYP compound I to be the lowest of the three systems. However, the thiolate ligated P450 was found to have the same oxygen spin population within error as its selenolate counterpart. This result is at odds with resonance Raman studies which clearly demonstrate the increased donating ability of SeP450 over the native system.[63,64] While more experiments are necessary to identify the origin of this discrepancy, a key reason could come from the analysis of the ENDOR hyperfine anisotropy. Compound I of the selenolate ligated P450 exhibited a highly rhombic hyperfine tensor, which indicates that the populations of the oxygen P_x and P_y orbitals are substantially different which may be a result of the greater π-donation of the selenolate. Taken together, these studies highlight the impact pK_a can have on the strength of C–H bonds that metal-oxidos can activate. Moreover, they reveal that tuning of the pK_a can be achieved through subtle interactions like H-bonds involving the oxido and/or axial ligand.

Offsetting the need for a high potential intermediate through an increase in the pK_a will obviously also alter the contributions of the PT and ET energetics to the C–H bond activation process (eq 1, Figure 2). Accordingly, it will affect both the rate and mechanism with the propensity for passing through an imbalanced transition state, but this remains to be shown in a biological context. Although tuning of the pK_a and mechanism through changes to the H-bond interactions of the axial ligand of P450 is an alluring approach, it would require detailed studies to systematically tune the strength of single hydrogen bond in such a complex biological setting. Another approach to studying this concept is using synthetic complexes: bioinspired coordination complexes have advantages and can offer key insights, as their ligands are often modular and can be rationally modified to alter the strength of H-bonding interactions.

Synthetic Complexes

Our group has shown that it is possible to emulate this strategy employed by biology and prepared Fe^{III} and Mn^{III} complexes baring basic metal-oxido units for the activation of C–H bonds.[22,23,48,65]In particular, in a variation of our tripodal ligand, $[H_3buea]^{3-}$, we prepared the $[Mn^{III}H_3buea(O)]^{2-}$ complex (Figure 4A) that showed reactivity toward dihydroxyanthracene (DHA) despite a redox potential that is bounded at −2.0 V versus $[Fe^{III/II}Cp_2]^{+/0}$, a potential that is similar to decamethylcobaltocene (−1.94 vs versus $[Fe^{III/II}Cp_2]^{+/0}$) which is a well-known reductant. Based on the electrochemical potential alone, the Mn^{III}–oxido complex should not be expected to perform oxidative cleavage

of C–H bonds, however its conjugate acid, the Mn^{III}–OH complex, $[Mn^{III}H_3buea(OH)]^-$, compensates for the negative potential with a sufficiently high pK_a of ~28 that was experimentally measured in DMSO. This p*K*a is greater than 15 units higher than that of the corresponding Fe^{IV}-hydroxido counterpart, $[Fe^{IV}H_3buea(OH)]^-$, that demonstrated negligible towards DHA.[47,66] With the exception of a slightly shorter M=O bond by 0.1 Å in the case of Mn, the molecular structures of $[Mn^{III}H_3buea(O)]^{2-}$ and $[Fe^{IV}H_3buea(O)]^-$ complexes are nearly isomorphic and both compounds exhibit EPR spectra consistent with the assignment of S=2 ground states (Figure 4). Together these results suggest that the differences in reactivity between these two complexes arises from their relative basicity. Moreover, a key difference between the Mn^{III} and Fe^{IV} oxido complexes is their charge. While the nonpolar nature of the substrate makes any differences in stabilization of substrate through electrostatics unlikely, it is reasonable that the increased effective nuclear charge of the metal center upon going from the Mn^{III} to Fe^{IV} provides increased stability to the oxido ligand, resulting in a decrease the relative pK_a of the Fe^{IV}–OH complex.

As previously discussed, both electron donation and oxygen spin population have been proposed as key components that in C–H bond cleavage. It was further experimentally determined through analyses of the hyperfine coupling of ^{17}O-enriched samples by electron paramagnetic resonance (EPR) spectroscopy that the Mn^{III}–oxido complex exhibited significantly less spin-density residing on the oxido ligand than the Fe^{IV}-oxido complex. We found that the less reactive Fe complex exhibits both a lower pK_a and higher an oxygen spin population (ρ_π) of 0.56 compared to the more basic and more reactive Mn complex that displays a decreased ρ_π of 0.30. Note that these results agree with the findings of Field and Green in that reactivity and spin-density have an inverse correlation with charge-density on the terminal oxido (that is, more reactivity systems are basic and have lower spin populations).

The demonstration of the importance of metal-oxido basicity prompted us to investigate the degree to which modulating the basicity of our Mn oxido complexes could influence reactivity. One advantage of our ligand frameworks is their modular nature and ability to regulate the secondary coordination sphere of the metal center through the incorporation of intramolecular H-bonds. We were therefore able to redesign the $[H_3buea]^{3-}$ complexes to incorporate a single tripodal arm exhibiting a para-substituted phenylurea group whereby he substituents in the *para* position were varied, $[Mn^{III}H_3bpuea\text{-}R(O)]^{2-}$ (Figure 5).[23] Systematic changes in the R-group modified the H-bond strength of the unique NH group to the oxido unit, which tuned the basicity of the metal-oxido complex and allowed us to examine the impact these changes had on reactivity. Through this approach we modulate the pK_a by >2 units, but found a lack of linear correlation between the second-order rate constants and the $BDFC_{C–H}$ of DHA; these results suggested a deviation from BEP-behavior and a CPET mechanism. Although, we did find substantially better correlation of log(k) with the pK_a($Mn^{III}OH$) values, our combined results did not support a stepwise mechanism involving rate-limiting proton transfer. For example, while xanthene and DHA exhibit similar pK_a values of their respective C–H bonds, their second order rate constants were substantially different. We are not alone in finding discrepancies in rate data for C–H cleavage process by metal-oxido complexes.[18,20,24,28,30] For instance, Anderson has

reported that the rates of reactivity of his CO^{III}-oxido complex deviate from a BEP-type relationship in favor of a good correlation between $\log(k_{obs})$ and the pK_a(C–H) values from the C–H bonds of the substrates.[27] Like the Mn^{III}–oxido complexes, this Co^{III}–oxido complex is strongly basic ($pK_a(Mn^{II}OH)$ of ~15 in DMSO),[27] leading in both cases to mechanistic suggestions that favor proton transfer (PT)-dominated imbalanced transition states (Figure 2F). In addition, Anderson has explored imbalanced transition states in the context of his complexes that includes a theoretical treatment of asynchronous mechanisms involving metal-oxido C–H bond.[20,25]

We have also further explored this possibility of non-BEP behavior in our Mn^{IV}-oxido complex, $[Mn^{IV}H_3buea(O)]^-$, which allowed us to examine a wider variety of substrates. One noticeable finding was the large spread of ~10^4 in the value of the second order rate constants that trended with increasing acidity of the C–H bond. However, there were again inconsistencies in the trend that precluded the assignment of a two-step mechanism, such as a large disparity between the second order rate constants of xanthene and DHA. Based on the observation that the basicity of our complexes played an important role in their reactivity, we further considered whether our compounds were passing through a PT-dominated imbalanced transition state. When contributions of ΔG°_{PT} and ΔG°_{ET} to the transition state are equal, synchronous transfer of the proton and electron is expected and the reaction barrier, $\Delta G^{\circ\ddagger}_{syn}$, is proportional to the driving force for the CPET process, ΔG°_{CPET} (eqs 2-4, Figure 2A). Recognizing that when the free energy contributions

$$\Delta G^{\circ\ddagger}_{syn} = \alpha(\Delta G^\circ_{CPET}) + \beta \quad (2)$$

$$\Delta G^\circ_{CPET} = \Delta G^\circ_{PT} + \Delta G^\circ_{ET} \quad (3)$$

of the PT and ET processes are not equal, we expect deviations from a linear relationship of the BDFE, described by $\Delta G^\circ_{PT} + \Delta G^\circ_{ET}$, with the second order rate constant (Figure 2D-F). We therefore reasoned that a modified version of the eq 4 that accounts for the differing PT and ET contributions to the transition state would be better suited to model our results. This insight led to eq 5 and we utilized it to developed a semi-empirical method to evaluate the degree of imbalance.[22] In this method, a PT-dominated process would show linearity between $\log(k)$ and $(\Delta G^\circ_{PT} + x\,\Delta G^\circ_{ET})$, with x representing the relative degree of ET character and determination of the appropriate value of x is evaluated by maximizing the R^2 of the line of best fit to the data (Figure 6).

$$\Delta G^{\circ\ddagger}_{syn} = \alpha(\Delta G^\circ_{PT} + \Delta G^\circ_{ET}) + \beta \quad (4)$$

$$\Delta G^{\circ\ddagger}_{asyn} = \alpha(\Delta G^\circ_{PT} + x\,\Delta G^\circ_{ET}) + \beta \quad (5)$$

From this analysis, we found that reactivity of $[Mn^{IV}H_3buea(O)]^-$ exhibited improved fits of $\log(k)$ to the driving force with scaled ET coefficients of 0.56. We believe this trend supports

our assignment of an asynchronous mechanism PT mechanism. The basicity is therefore found to provide a useful handle for altering the rate and influencing the mechanism of C–H bond activation. We note that a similar correlation was observed with the Co^{III}–oxido system of Anderson; in this case, an ET coefficient of 0.45 was found.[22]

Conclusions and Future Directions

In recent years, the impact of the basicity of transition metal oxidos PCET reactions has garnered increasing attention as attractive strategy for activating increasingly strong C–H bonds while mitigating the need for excessively high redox potentials. The basicity of a metal-oxido unit can be influenced by a variety of factors in the primary coordination sphere including the degree of covalency or donating ability of the ligands as well as non-covalent interactions in the secondary coordination sphere. Of the second coordination sphere factors, H-bonds have emerged as useful interactions to regulate functional properties and their ubiquity within the active sites of metalloprotein provides evidence for their importance. Within the context of C–H bond functionalization, there is a need for more experimental support for mechanistic ramification of H-bond, especially a quantitative assessment of the extent to which H-bonds can influence the degree of imbalance in a transition state.

We use this Frontier as an opportunity to suggest two areas for development in this area. First, as we have highlighted here with the incorporation of selenocysteine as axial ligands cytochrome P450s, the utility of noncanonical amino acids is a powerful potential avenue for the study of the influence of the strengths that H-bonds may have reactivity. Similar approaches have shown their utilized in synthetic systems: we have demonstrated how the systematic modification of single H-bond donating group within a Mn-oxido can regulated the rate of C–H bond activation. In analogy to this, protein systems could be developed that incorporate non-canonical tyrosine derivatives into metalloenzymes that interact directly with the metal-oxido unit, or via an axial ligand like the H-bonding network formed in P450s (Figure 7A). In doing so, one can systematic tune the strength of a single H-bond and examine its effect on metal oxido basicity in a complex biological environment. A similar approach was recently taken in the study of a HAT by a nonheme iron (NHFe) endoperoxidase, verruculogen synthase (FtmOx1) where the authors incorporate ring-halogenated tyrosine derivatives to aid in the identification of the tyrosine responsible for controlling radical reactivity in the synthesis of the natural product, verruculogen.[67]

A second approach takes advantage of the advances of X-ray spectroscopy techniques at synchrotrons and x-ray free electron lasers (XFELs) that enable real-time observation of electronic state changes in enzymatic metallocofactors.[68–80] K-edge X-ray absorption/emission spectroscopies (XAS/XES) are powerful techniques for studying the protonation states of transition metal oxidos as they are element selective and highly sensitive to the local electronic and geometric structure of the metal center. Three cases illustrate the utility and promise of these methods in which K-edge X-ray emission spectroscopy was applied to determine the protonation states of the oxido ligands of dinuclear Mn^{IV}, Ca complexes, and the Mn_4Ca cofactor of photosystem II respectively.[73,81,82] In particular, emission lines arising from valence-to-core (VtC) transitions are exceptionally sensitive to features of transition metal ligands allowing for determination of important chemical properties like

ionization potential, protonation state, and hybridization.[73,76,81,83] Upon X-ray absorption at the metal K-edge, electrons are excited from the 1s orbital to continuum levels and when electrons from the ligand np or ns orbitals fall to fill the core hole created by the 1s excitation, X-rays are emitted giving rise to spectral features known as K $\beta_{2,5}$ and K β'', sometimes referred to as valence-to-core (VtC) transitions (Figure 7B). As the origin of the emission features reflect orbitals that have strong ligand *n*p and *n*s (and metal 3d) character, making them very sensitive to changes in the primary coordination sphere. Continued developments in both steady-state and time-resolved versions of these techniques will open exciting opportunities to study challenging chemical mechanisms with unprecedented temporal and spectral resolution especially when combined with structural information.

Acknowledgements.

The authors acknowledge the NIH (GM050781 and GM120349 to A.S.B.) for financial support.

References

(1). Gunay A; Theopold KH C–H Bond Activations by Metal Oxo Compounds. Chem. Rev 2010, 110 (2), 1060–1081. 10.1021/cr900269x. [PubMed: 20143877]

(2). Lee JL; Ross DL; Barman SK; Ziller JW; Borovik AS C–H Bond Cleavage by Bioinspired Nonheme Metal Complexes. Inorg. Chem 2021, 60 (18), 13759–13783. 10.1021/acs.inorgchem.1c01754. [PubMed: 34491738]

(3). Lewis JC; Coelho PS; Arnold FH Enzymatic Functionalization of Carbon–Hydrogen Bonds. Chem. Soc. Rev 2011, 40 (4), 2003–2021. 10.1039/C0CS00067A. [PubMed: 21079862]

(4). Stone KL; Borovik A Lessons from Nature: Unraveling Biological CH Bond Activation. Current Opinion in Chemical Biology 2009, 13 (1), 114–118. 10.1016/j.cbpa.2009.02.008. [PubMed: 19297238]

(5). Huang X; Groves JT Oxygen Activation and Radical Transformations in Heme Proteins and Metalloporphyrins. Chem. Rev 2018, 118 (5), 2491–2553. 10.1021/acs.chemrev.7b00373. [PubMed: 29286645]

(6). Poulos TL Heme Enzyme Structure and Function. Chemical Reviews 2014, 114 (7), 3919–3962. 10.1021/cr400415k. [PubMed: 24400737]

(7). Costas M; Mehn MP; Jensen MP; Que L Dioxygen Activation at Mononuclear Nonheme Iron Active Sites: Enzymes, Models, and Intermediates. Chem. Rev 2004, 104 (2), 939–986. 10.1021/cr020628n. [PubMed: 14871146]

(8). Bordwell FG Equilibrium Acidities in Dimethyl Sulfoxide Solution. Acc. Chem. Res 1988, 21 (12), 456–463. 10.1021/ar00156a004.

(9). Bordwell FG; Cheng J; Ji GZ; Satish AV; Zhang X Bond Dissociation Energies in DMSO Related to the Gas Phase Values. J. Am. Chem. Soc 1991, 113 (26), 9790–9795. 10.1021/ja00026a012.

(10). Parker VD; Handoo KL; Roness F; Tilset M Electrode Potentials and the Thermodynamics of Isodesmic Reactions. J. Am. Chem. Soc 1991, 113 (20), 7493–7498. 10.1021/ja00020a007.

(11). Warren JJ; Tronic TA; Mayer JM Thermochemistry of Proton-Coupled Electron Transfer Reagents and Its Implications. Chem. Rev 2010, 110 (12), 6961–7001. 10.1021/cr100085k. [PubMed: 20925411]

(12). Mayer JM PROTON-COUPLED ELECTRON TRANSFER: A Reaction Chemist's View. Annu. Rev. Phys. Chem 2004, 55 (1), 363–390. 10.1146/annurev.physchem.55.091602.094446. [PubMed: 15117257]

(13). Tyburski R; Liu T; Glover SD; Hammarström L Proton-Coupled Electron Transfer Guidelines, Fair and Square. J. Am. Chem. Soc 2021, 143 (2), 560–576. 10.1021/jacs.0c09106. [PubMed: 33405896]

(14). Hammes-Schiffer S; Stuchebrukhov AA Theory of Coupled Electron and Proton Transfer Reactions. Chem. Rev 2010, 110 (12), 6939–6960. 10.1021/cr1001436. [PubMed: 21049940]

(15). Cukier RI; Nocera DG PROTON-COUPLED ELECTRON TRANSFER. Annu. Rev. Phys. Chem 1998, 49 (1), 337–369. 10.1146/annurev.physchem.49.1.337. [PubMed: 9933908]

(16). Reece SY; Nocera DG Proton-Coupled Electron Transfer in Biology: Results from Synergistic Studies in Natural and Model Systems. Annu. Rev. Biochem 2009, 78 (1), 673–699. 10.1146/annurev.biochem.78.080207.092132. [PubMed: 19344235]

(17). Darcy JW; Koronkiewicz B; Parada GA; Mayer JM A Continuum of Proton-Coupled Electron Transfer Reactivity. Acc. Chem. Res 2018, 51 (10), 2391–2399. 10.1021/acs.accounts.8b00319. [PubMed: 30234963]

(18). Coste SC; Brezny AC; Koronkiewicz B; Mayer JM C–H Oxidation in Fluorenyl Benzoates Does Not Proceed through a Stepwise Pathway: Revisiting Asynchronous Proton-Coupled Electron Transfer. Chem. Sci 2021, 12 (39), 13127–13136. 10.1039/D1SC03344A. [PubMed: 34745543]

(19). Hodgkiss JM; Rosenthal J; Nocera DG The Relation between Hydrogen Atom Transfer and Proton-Coupled Electron Transfer in Model Systems. In Hydrogen-Transfer Reactions; Hynes JT, Klinman JP, Limbach H-H, Schowen RL, Eds.; Wiley-VCH Verlag GmbH & Co. KGaA: Weinheim, Germany, 2006; pp 503–562. 10.1002/9783527611546.ch17.

(20). Bím D; Maldonado-Domínguez M; Rulíšek L; Srnec M Beyond the Classical Thermodynamic Contributions to Hydrogen Atom Abstraction Reactivity. Proc. Natl. Acad. Sci. U.S.A 2018, 115 (44). 10.1073/pnas.1806399115.

(21). Goings JJ; Hammes-Schiffer S Nonequilibrium Dynamics of Proton-Coupled Electron Transfer in Proton Wires: Concerted but Asynchronous Mechanisms. ACS Cent. Sci 2020, 6 (9), 1594–1601. 10.1021/acscentsci.0c00756. [PubMed: 32999935]

(22). Barman SK; Yang M-Y; Parsell TH; Green MT; Borovik AS Semiempirical Method for Examining Asynchronicity in Metal–Oxido-Mediated C–H Bond Activation. Proc. Natl. Acad. Sci. U.S.A 2021, 118 (36), e2108648118. 10.1073/pnas.2108648118. [PubMed: 34465626]

(23). Barman SK; Jones JR; Sun C; Hill EA; Ziller JW; Borovik AS Regulating the Basicity of Metal–Oxido Complexes with a Single Hydrogen Bond and Its Effect on C–H Bond Cleavage. J. Am. Chem. Soc 2019, 141 (28), 11142–11150. 10.1021/jacs.9b03688. [PubMed: 31274298]

(24). Bower JK; Reese MS; Mazin IM; Zarnitsa LM; Cypcar AD; Moore CE; Sokolov A. Yu.; Zhang S C(Sp^3)–H Cyanation by a Formal Copper(III) Cyanide Complex. Chem. Sci 2023, 14 (5), 1301–1307. 10.1039/D2SC06573H. [PubMed: 36756315]

(25). Schneider JE; Goetz MK; Anderson JS Reconciling Off-Diagonal Thermodynamic Effects with Nonadiabatic CPET Reactions.

(26). Schneider JE; Goetz MK; Anderson JS Statistical Analysis of C–H Activation by Oxo Complexes Supports Diverse Thermodynamic Control over Reactivity. Chem. Sci 2021, 12 (11), 4173–4183. 10.1039/D0SC06058E. [PubMed: 34163690]

(27). Zhao N; Goetz M; Schneider J; Anderson J Testing the Limits of Imbalanced CPET Reactivity: Mechanistic Crossover in H-Atom Abstraction by Co(III)-Oxo Complexes; preprint; Chemistry, 2022. 10.26434/chemrxiv-2022-7fkj9.

(28). Kotani H; Shimomura H; Ikeda K; Ishizuka T; Shiota Y; Yoshizawa K; Kojima T Mechanistic Insight into Concerted Proton–Electron Transfer of a Ru(IV)-Oxo Complex: A Possible Oxidative Asynchronicity. J. Am. Chem. Soc 2020, 142 (40), 16982–16989. 10.1021/jacs.0c05738. [PubMed: 32924508]

(29). Costentin C; Savéant J-M Hydrogen and Proton Exchange at Carbon. Imbalanced Transition State and Mechanism Crossover. Chem. Sci 2020, 11 (4), 1006–1010. 10.1039/C9SC05147C.

(30). Elwell CE; Mandal M; Bouchey CJ; Que L; Cramer CJ; Tolman WB Carboxylate Structural Effects on the Properties and Proton-Coupled Electron Transfer Reactivity of [CuO_2 CR] $^{2+}$ Cores. Inorg. Chem 2019, 58 (23), 15872–15879. 10.1021/acs.inorgchem.9b02293. [PubMed: 31710477]

(31). Bernasconi CF The Principle of Non-Perfect Synchronization. In Advances in Physical Organic Chemistry; Elsevier, 1992; Vol. 27, pp 119–238. 10.1016/S0065-3160(08)60065-9.

(32). Tishchenko O; Truhlar DG; Ceulemans A; Nguyen MT A Unified Perspective on the Hydrogen Atom Transfer and Proton-Coupled Electron Transfer Mechanisms in Terms of Topographic Features of the Ground and Excited Potential Energy Surfaces As Exemplified by the Reaction

between Phenol and Radicals. J. Am. Chem. Soc 2008, 130 (22), 7000–7010. 10.1021/ja7102907. [PubMed: 18465862]

(33). Hydrogen-Transfer Reactions, 1st ed.; Hynes JT, Klinman JP, Limbach H, Schowen RL, Eds.; Wiley, 2006. 10.1002/9783527611546.

(34). Wang D; Ray K; Collins MJ; Farquhar ER; Frisch JR; Gómez L; Jackson TA; Kerscher M; Waleska A; Comba P; Costas M; Que L Nonheme Oxoiron(IV) Complexes of Pentadentate N5 Ligands: Spectroscopy, Electrochemistry, and Oxidative Reactivity. Chem. Sci 2013, 4 (1), 282–291. 10.1039/C2SC21318D. [PubMed: 23227304]

(35). Bigi JP; Harman WH; Lassalle-Kaiser B; Robles DM; Stich TA; Yano J; Britt RD; Chang CJ A High-Spin Iron(IV)–Oxo Complex Supported by a Trigonal Nonheme Pyrrolide Platform. J. Am. Chem. Soc 2012, 134 (3), 1536–1542. 10.1021/ja207048h. [PubMed: 22214221]

(36). Hong S; Lee Y-M; Cho K-B; Sundaravel K; Cho J; Kim MJ; Shin W; Nam W Ligand Topology Effect on the Reactivity of a Mononuclear Nonheme Iron(IV)-Oxo Complex in Oxygenation Reactions. J. Am. Chem. Soc 2011, 133 (31), 11876–11879. 10.1021/ja204008u. [PubMed: 21736350]

(37). Sacramento JJD; Goldberg DP Factors Affecting Hydrogen Atom Transfer Reactivity of Metal–Oxo Porphyrinoid Complexes. Acc. Chem. Res 2018, 51 (11), 2641–2652. 10.1021/acs.accounts.8b00414. [PubMed: 30403479]

(38). Ehudin MA; Quist DA; Karlin KD Enhanced Rates of C–H Bond Cleavage by a Hydrogen-Bonded Synthetic Heme High-Valent Iron(IV) Oxo Complex. J. Am. Chem. Soc 2019, 141 (32), 12558–12569. 10.1021/jacs.9b01253. [PubMed: 31318198]

(39). Dantignana V; Serrano-Plana J; Draksharapu A; Magallón C; Banerjee S; Fan R; Gamba I; Guo Y; Que L; Costas M; Company A Spectroscopic and Reactivity Comparisons between Nonheme Oxoiron(IV) and Oxoiron(V) Species Bearing the Same Ancillary Ligand. J. Am. Chem. Soc 2019, 141 (38), 15078–15091. 10.1021/jacs.9b05758. [PubMed: 31469954]

(40). Kupper C; Mondal B; Serrano-Plana J; Klawitter I; Neese F; Costas M; Ye S; Meyer F Nonclassical Single-State Reactivity of an Oxo-Iron(IV) Complex Confined to Triplet Pathways. J. Am. Chem. Soc 2017, 139 (26), 8939–8949. 10.1021/jacs.7b03255. [PubMed: 28557448]

(41). Seo MS; Kim NH; Cho K-B; So JE; Park SK; Clémancey M; Garcia-Serres R; Latour J-M; Shaik S; Nam W A Mononuclear Nonheme Iron(Iv)-Oxo Complex Which Is More Reactive than Cytochrome P450 Model Compound I. Chem. Sci 2011, 2 (6), 1039. 10.1039/c1sc00062d.

(42). Bell RP The Theory of Reactions Involving Proton Transfers. Proc. R. Soc. Lond. A 1936, 154 (882), 414–429. 10.1098/rspa.1936.0060.

(43). Evans MG; Polanyi M Inertia and Driving Force of Chemical Reactions. Trans. Faraday Soc 1938, 34, 11. 10.1039/tf9383400011.

(44). Mittra K; Green MT Reduction Potentials of P450 Compounds I and II: Insight into the Thermodynamics of C–H Bond Activation. J. Am. Chem. Soc 2019, 141 (13), 5504–5510. 10.1021/jacs.9b00242. [PubMed: 30892878]

(45). Yosca TH; Rittle J; Krest CM; Onderko EL; Silakov A; Calixto JC; Behan RK; Green MT Iron(IV)Hydroxide p K_a and the Role of Thiolate Ligation in C–H Bond Activation by Cytochrome P450. Science 2013, 342 (6160), 825–829. 10.1126/science.1244373. [PubMed: 24233717]

(46). Green MT; Dawson JH; Gray HB Oxoiron(IV) in Chloroperoxidase Compound II Is Basic: Implications for P450 Chemistry. Science 2004, 304 (5677), 1653–1656. 10.1126/science.1096897. [PubMed: 15192224]

(47). Usharani D; Lacy DC; Borovik AS; Shaik S Dichotomous Hydrogen Atom Transfer vs Proton-Coupled Electron Transfer During Activation of X–H Bonds (X = C, N, O) by Nonheme Iron–Oxo Complexes of Variable Basicity. J. Am. Chem. Soc 2013, 135 (45), 17090–17104. 10.1021/ja408073m. [PubMed: 24124906]

(48). Parsell TH; Yang M-Y; Borovik AS C–H Bond Cleavage with Reductants: Re-Investigating the Reactivity of Monomeric Mn $^{III/IV}$ –Oxo Complexes and the Role of Oxo Ligand Basicity. J. Am. Chem. Soc 2009, 131 (8), 2762–2763. 10.1021/ja8100825. [PubMed: 19196005]

(49). Rittle J; Green MT Cytochrome P450 Compound I: Capture, Characterization, and C-H Bond Activation Kinetics. Science 2010, 330 (6006), 933. 10.1126/science.1193478. [PubMed: 21071661]

(50). Denisov IG; Sligar SG Activation of Molecular Oxygen in Cytochromes P450. In Cytochrome P450; Ortiz De Montellano PR, Ed.; Springer International Publishing: Cham, 2015; pp 69–109. 10.1007/978-3-319-12108-6_3.

(51). Poulos TL; Follmer AH Updating the Paradigm: Redox Partner Binding and Conformational Dynamics in Cytochromes P450. Acc. Chem. Res 2022, 55 (3), 373–380. 10.1021/acs.accounts.1c00632. [PubMed: 34965086]

(52). Behan RK; Green MT On the Status of Ferryl Protonation. Journal of Inorganic Biochemistry 2006, 100 (4), 448–459. 10.1016/j.jinorgbio.2005.12.019. [PubMed: 16500711]

(53). Aldag C; Gromov IA; Garcia-Rubio I; von Koenig K; Schlichting I; Jaun B; Hilvert D Probing the Role of the Proximal Heme Ligand in Cytochrome P450cam by Recombinant Incorporation of Selenocysteine. Proceedings of the National Academy of Sciences 2009, 106 (14), 5481–5486. 10.1073/pnas.0810503106.

(54). Onderko EL; Silakov A; Yosca TH; Green MT Characterization of a Selenocysteine-Ligated P450 Compound I Reveals Direct Link between Electron Donation and Reactivity. Nature Chem 2017, 9 (7), 623–628. 10.1038/nchem.2781. [PubMed: 28644466]

(55). Field MJ; Oyala PH; Green MT ^{17} O Electron Nuclear Double Resonance Analysis of Compound I: Inverse Correlation between Oxygen Spin Population and Electron Donation. J. Am. Chem. Soc 2022, 144 (42), 19272–19283. 10.1021/jacs.2c05459. [PubMed: 36240444]

(56). Yosca TH; Behan RK; Krest CM; Onderko EL; Langston MC; Green MT Setting an Upper Limit on the Myoglobin Iron(IV)Hydroxide p K a: Insight into Axial Ligand Tuning in Heme Protein Catalysis. Journal of the American Chemical Society 2014, 136 (25), 9124–9131. 10.1021/ja503588n. [PubMed: 24875119]

(57). Krest CM; Silakov A; Rittle J; Yosca TH; Onderko EL; Calixto JC; Green MT Significantly Shorter Fe–S Bond in Cytochrome P450-I Is Consistent with Greater Reactivity Relative to Chloroperoxidase. Nature Chem 2015, 7 (9), 696–702. 10.1038/nchem.2306. [PubMed: 26291940]

(58). Shaik S; De Visser SP; Ogliaro F; Schwarz H; Schröder D Two-State Reactivity Mechanisms of Hydroxylation and Epoxidation by Cytochrome P-450 Revealed by Theory. Current Opinion in Chemical Biology 2002, 6 (5), 556–567. 10.1016/S13675931(02)00363-0. [PubMed: 12413538]

(59). Hirao H; Kumar D; Thiel W; Shaik S Two States and Two More in the Mechanisms of Hydroxylation and Epoxidation by Cytochrome P450. J. Am. Chem. Soc 2005, 127 (37), 13007–13018. 10.1021/ja053847+. [PubMed: 16159296]

(60). Vandemeulebroucke A; Aldag C; Stiebritz MT; Reiher M; Hilvert D Kinetic Consequences of Introducing a Proximal Selenocysteine Ligand into Cytochrome P450cam. Biochemistry 2015, 54 (44), 6692–6703. 10.1021/acs.biochem.5b00939. [PubMed: 26460790]

(61). Dietl N; Schlangen M; Schwarz H Thermal Hydrogen-Atom Transfer from Methane: The Role of Radicals and Spin States in Oxo-Cluster Chemistry. Angew. Chem. Int. Ed 2012, 51 (23), 5544–5555. 10.1002/anie.201108363.

(62). Saouma CT; Mayer JM Do Spin State and Spin Density Affect Hydrogen Atom Transfer Reactivity? Chem. Sci 2014, 5 (1), 21–31. 10.1039/C3SC52664J.

(63). Jiang Y; Sivaramakrishnan S; Hayashi T; Cohen S; Moënne-Loccoz P; Shaik S; Ortiz de Montellano PR Calculated and Experimental Spin State of Seleno Cytochrome P450. Angew. Chem. Int. Ed 2009, 48 (39), 7193–7195. 10.1002/anie.200901485.

(64). Hu S; Kincaid JR Heme Active-Site Structural Characterization of Chloroperoxidase by Resonance Raman Spectroscopy. Journal of Biological Chemistry 1993, 268 (9), 6189–6193. 10.1016/S0021-9258(18)53237-3. [PubMed: 8384203]

(65). Gupta R; Borovik AS Monomeric Mn $^{III/II}$ and Fe $^{III/II}$ Complexes with Terminal Hydroxo and Oxo Ligands: Probing Reactivity via O–H Bond Dissociation Energies. J. Am. Chem. Soc 2003, 125 (43), 13234–13242. 10.1021/ja0301491. [PubMed: 14570499]

(66). Hill EA; Weitz AC; Onderko E; Romero-Rivera A; Guo Y; Swart M; Bominaar EL; Green MT; Hendrich MP; Lacy DC; Borovik AS Reactivity of an FeIV-Oxo Complex with Protons

and Oxidants. Journal of the American Chemical Society 2016, 138 (40), 13143–13146. 10.1021/jacs.6b07633. [PubMed: 27647293]

(67). Lin C-Y; Muñoz Hernández AL; Laremore TN; Silakov A; Krebs C; Boal AK; Bollinger JM Use of Noncanonical Tyrosine Analogues to Probe Control of Radical Intermediates during Endoperoxide Installation by Verruculogen Synthase (FtmOx1). ACS Catal. 2022, 12 (12), 6968–6979. 10.1021/acscatal.2c01037. [PubMed: 37744570]

(68). Bergmann U; Kern J; Schoenlein RW; Wernet P; Yachandra VK; Yano J Using X-Ray Free-Electron Lasers for Spectroscopy of Molecular Catalysts and Metalloenzymes. Nat Rev Phys 2021, 3 (4), 264–282. 10.1038/s42254-021-00289-3. [PubMed: 34212130]

(69). Kubin M; Kern J; Gul S; Kroll T; Chatterjee R; Löchel H; Fuller FD; Sierra RG; Quevedo W; Weniger C; Rehanek J; Firsov A; Laksmono H; Weninger C; Alonso-Mori R; Nordlund DL; Lassalle-Kaiser B; Glownia JM; Krzywinski J; Moeller S; Turner JJ; Minitti MP; Dakovski GL; Koroidov S; Kawde A; Kanady JS; Tsui EY; Suseno S; Han Z; Hill E; Taguchi T; Borovik AS; Agapie T; Messinger J; Erko A; Föhlisch A; Bergmann U; Mitzner R; Yachandra VK; Yano J; Wernet P Soft X-Ray Absorption Spectroscopy of Metalloproteins and High-Valent Metal-Complexes at Room Temperature Using Free-Electron Lasers. Structural Dynamics 2017, 4 (5), 054307. 10.1063/1.4986627. [PubMed: 28944255]

(70). Mitzner R; Rehanek J; Kern J; Gul S; Hattne J; Taguchi T; Alonso-Mori R; Tran R; Weniger C; Schröder H; Quevedo W; Laksmono H; Sierra RG; Han G; Lassalle-Kaiser B; Koroidov S; Kubicek K; Schreck S; Kunnus K; Brzhezinskaya M; Firsov A; Minitti MP; Turner JJ; Moeller S; Sauter NK; Bogan MJ; Nordlund D; Schlotter WF; Messinger J; Borovik A; Techert S; de Groot FMF; Föhlisch A; Erko A; Bergmann U; Yachandra VK; Wernet P; Yano J L-Edge X-Ray Absorption Spectroscopy of Dilute Systems Relevant to Metalloproteins Using an X-Ray Free-Electron Laser. J. Phys. Chem. Lett 2013, 4 (21), 3641–3647. 10.1021/jz401837f. [PubMed: 24466387]

(71). Lassalle-Kaiser B; Boron TT; Krewald V; Kern J; Beckwith MA; Delgado-Jaime MU; Schroeder H; Alonso-Mori R; Nordlund D; Weng T-C; Sokaras D; Neese F; Bergmann U; Yachandra VK; DeBeer S; Pecoraro VL; Yano J Experimental and Computational X-Ray Emission Spectroscopy as a Direct Probe of Protonation States in Oxo-Bridged Mn ^{IV} Dimers Relevant to Redox-Active Metalloproteins. Inorg. Chem 2013, 52 (22), 12915–12922. 10.1021/ic400821g. [PubMed: 24161081]

(72). Pollock CJ; Delgado-Jaime MU; Atanasov M; Neese F; DeBeer S Kβ Mainline X-Ray Emission Spectroscopy as an Experimental Probe of Metal–Ligand Covalency. J. Am. Chem. Soc 2014, 136 (26), 9453–9463. 10.1021/ja504182n. [PubMed: 24914450]

(73). Martinie RJ; Blaesi EJ; Bollinger JM; Krebs C; Finkelstein KD; Pollock CJ Two-Color Valence-to-Core X-ray Emission Spectroscopy Tracks Cofactor Protonation State in a Class I Ribonucleotide Reductase. Angew. Chem 2018, 130 (39), 12936–12940. 10.1002/ange.201807366.

(74). Fuller FD; Gul S; Chatterjee R; Burgie ES; Young ID; Lebrette H; Srinivas V; Brewster AS; Michels-Clark T; Clinger JA; Andi B; Ibrahim M; Pastor E; De Lichtenberg C; Hussein R; Pollock CJ; Zhang M; Stan CA; Kroll T; Fransson T; Weninger C; Kubin M; Aller P; Lassalle L; Bräuer P; Miller MD; Amin M; Koroidov S; Roessler CG; Allaire M; Sierra RG; Docker PT; Glownia JM; Nelson S; Koglin JE; Zhu D; Chollet M; Song S; Lemke H; Liang M; Sokaras D; Alonso-Mori R; Zouni A; Messinger J; Bergmann U; Boal AK; Bollinger JM; Krebs C; Högbom M; Phillips GN; Vierstra RD; Sauter NK; Orville AM; Kern J; Yachandra VK; Yano J Drop-on-Demand Sample Delivery for Studying Biocatalysts in Action at X-Ray Free-Electron Lasers. Nat Methods 2017, 14 (4), 443–449. 10.1038/nmeth.4195. [PubMed: 28250468]

(75). Mara MW; Hadt RG; Reinhard ME; Kroll T; Lim H; Hartsock RW; Alonso-Mori R; Chollet M; Glownia JM; Nelson S; Sokaras D; Kunnus K; Hodgson KO; Hedman B; Bergmann U; Gaffney KJ; Solomon EI Metalloprotein Entatic Control of Ligand-Metal Bonds Quantified by Ultrafast x-Ray Spectroscopy. Science 2017, 356 (6344), 1276–1280. 10.1126/science.aam6203. [PubMed: 28642436]

(76). Lim H; Baker ML; Cowley RE; Kim S; Bhadra M; Siegler MA; Kroll T; Sokaras D; Weng T-C; Biswas DR; Dooley DM; Karlin KD; Hedman B; Hodgson KO; Solomon EI Kβ X-Ray Emission Spectroscopy as a Probe of Cu(I) Sites: Application to the Cu(I) Site in Preprocessed Galactose

Oxidase. Inorg. Chem 2020, 59 (22), 16567–16581. 10.1021/acs.inorgchem.0c02495. [PubMed: 33136386]

(77). Reinhard ME; Mara MW; Kroll T; Lim H; Hadt RG; Alonso-Mori R; Chollet M; Glownia JM; Nelson S; Sokaras D; Kunnus K; Driel TBV; Hartsock RW; Kjaer KS; Weninger C; Biasin E; Gee LB; Hodgson KO; Hedman B; Bergmann U; Solomon EI; Gaffney KJ Short-Lived Metal-Centered Excited State Initiates Iron-Methionine Photodissociation in Ferrous Cytochrome c. Nat Commun 2021, 12 (1), 1086. 10.1038/s41467-021-21423-w. [PubMed: 33597529]

(78). Zhang W; Alonso-Mori R; Bergmann U; Bressler C; Chollet M; Galler A; Gawelda W; Hadt RG; Hartsock RW; Kroll T; Kjær KS; Kubiček K; Lemke HT; Liang HW; Meyer DA; Nielsen MM; Purser C; Robinson JS; Solomon EI; Sun Z; Sokaras D; van Driel TB; Vankó G; Weng T-C; Zhu D; Gaffney KJ Tracking Excited-State Charge and Spin Dynamics in Iron Coordination Complexes. Nature 2014, 509 (7500), 345–348. 10.1038/nature13252. [PubMed: 24805234]

(79). Miller NA; Michocki LB; Konar A; Alonso-Mori R; Deb A; Glownia JM; Sofferman DL; Song S; Kozlowski PM; Kubarych KJ; Penner-Hahn JE; Sension RJ Ultrafast XANES Monitors Femtosecond Sequential Structural Evolution in Photoexcited Coenzyme B_{12}. J. Phys. Chem. B 2020, 124 (1), 199–209. 10.1021/acs.jpcb.9b09286. [PubMed: 31850761]

(80). Chatterjee R; Weninger C; Loukianov A; Gul S; Fuller FD; Cheah MH; Fransson T; Pham CC; Nelson S; Song S; Britz A; Messinger J; Bergmann U; Alonso-Mori R; Yachandra VK; Kern J; Yano J XANES and EXAFS of Dilute Solutions of Transition Metals at XFELs. J Synchrotron Rad 2019, 26 (5), 1716–1724. 10.1107/S1600577519007550.

(81). Mathe Z; Pantazis DA; Lee HB; Gnewkow R; Van Kuiken BE; Agapie T; DeBeer S Calcium Valence-to-Core X-Ray Emission Spectroscopy: A Sensitive Probe of Oxo Protonation in Structural Models of the Oxygen-Evolving Complex. Inorg. Chem 2019, 58 (23), 16292–16301. 10.1021/acs.inorgchem.9b02866. [PubMed: 31743026]

(82). Pushkar Y; Long X; Glatzel P; Brudvig GW; Dismukes GC; Collins TJ; Yachandra VK; Yano J; Bergmann U Direct Detection of Oxygen Ligation to the Mn4Ca Cluster of Photosystem II by X-Ray Emission Spectroscopy. Angewandte Chemie International Edition 2010, 49 (4), 800–803. 10.1002/anie.200905366. [PubMed: 20017172]

(83). Schwalenstocker K; Paudel J; Kohn AW; Dong C; Van Heuvelen KM; Farquhar ER; Li F Cobalt Kβ Valence-to-Core X-Ray Emission Spectroscopy: A Study of Low-Spin Octahedral Cobalt(III) Complexes. Dalton Trans. 2016, 45 (36), 14191–14202. 10.1039/C6DT02413K. [PubMed: 27533922]

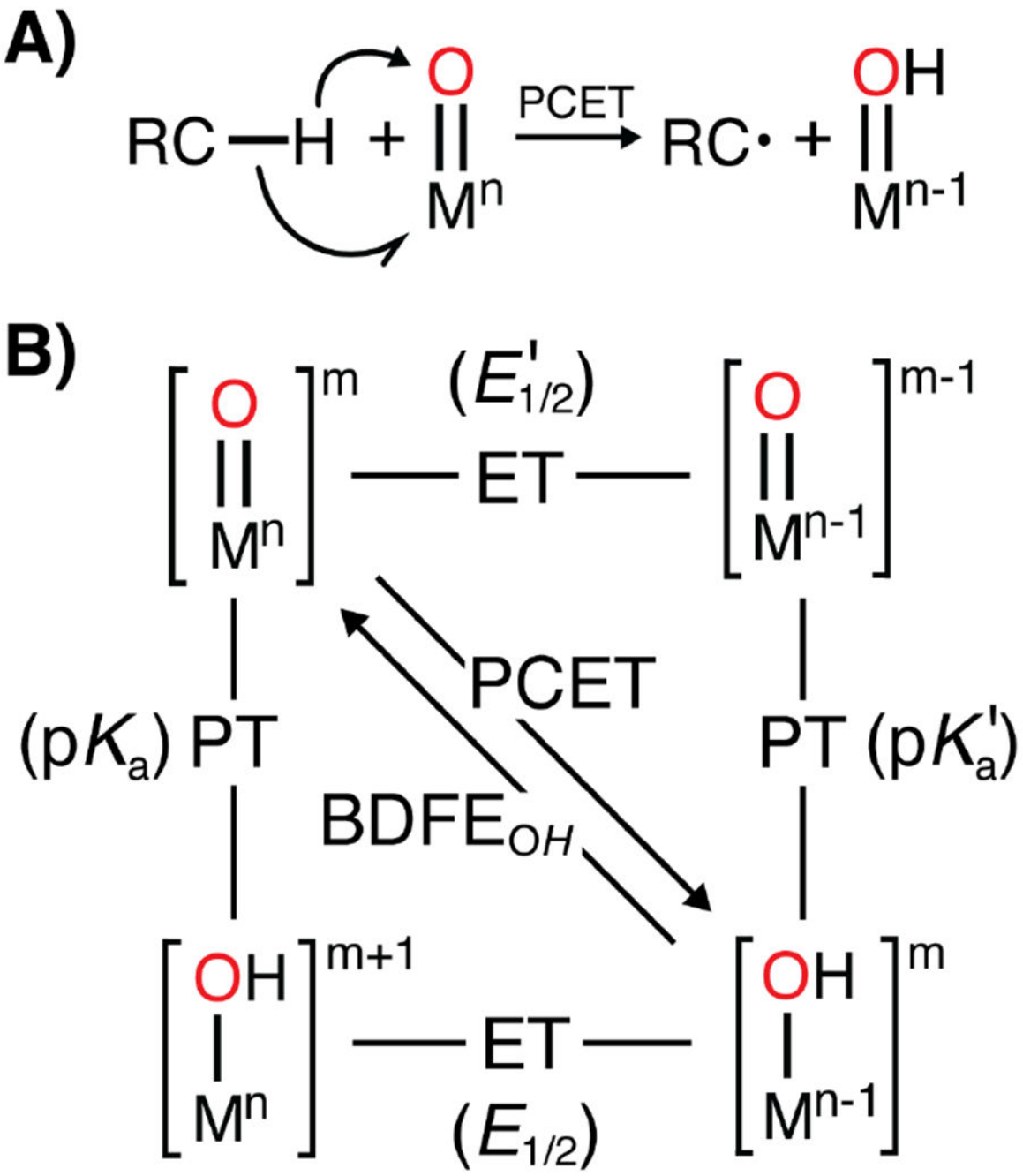

Figure 1.

(**A**) Activation scheme of C–H bond by a metal oxido complex. (**B**) Thermodynamic square scheme of potential HAT mechanisms by transitional metal-oxido complexes in C–H bond activation.

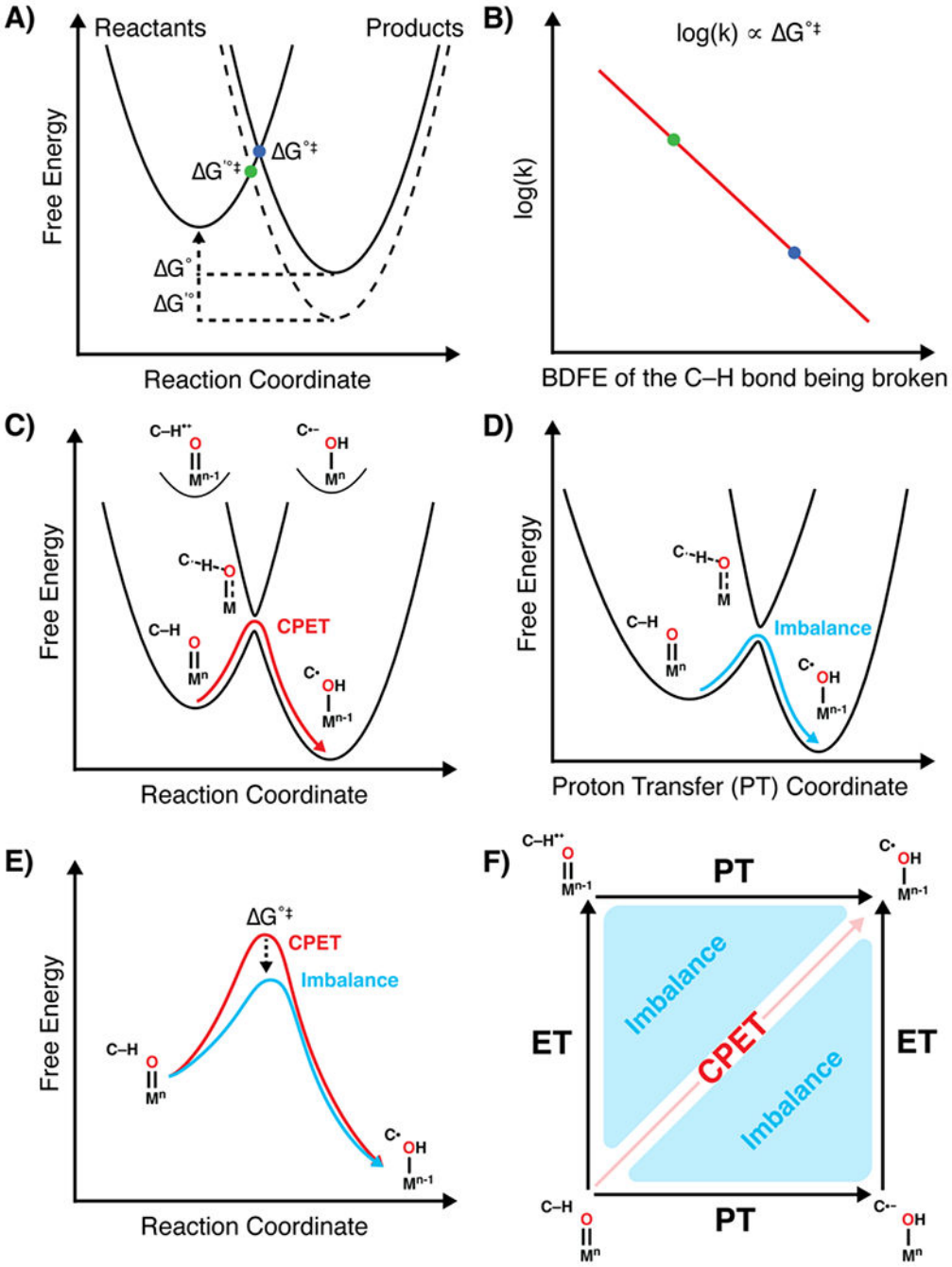

Figure 2.

(**A** and **B**) An illustration of the linear free energy relationship. Intersecting parabolas for a general PCET reaction demonstrating how a change in the driving force, Δ G, results in a proportional change in the energy of the transition state Δ $G^{‡}$. This results in a linear relationship between log(k) and the BDFE (Δ G) of the C–H bond, where k is the reaction rate constant. (**C**) The coupling of the proton and electron along the reaction coordinate in a PCET reaction results in an effective adiabatic double-well ground state potential for C–H bond activation. In a concerted proton electron transfer (CPET), the proton and electron

move effectively together through the transition state (TS) along this ground-state potential (red curve). Stepwise intermediates of the HAT reaction are shown as vertical transitions above reactant and product minima representing higher energy minima of on the same ground state surface. (**D**) In reactions where the proton and electron are coupled but do not move synchronously along the reaction coordinate, the TS becomes imbalanced (blue curve) visualized by projection along the proton transfer (PT) coordinate. In this example, the TS is PT-dominated compared to CPET. (**E**) A comparison of concerted and imbalanced PCET reactions demonstrating how reactions with equivalent thermodynamic properties result in different rates depending on the nature of the transition state. (**F**) A More O'Ferrell-Jencks plot with step-wise ET-PT and PT-ET mechanisms along ET and PT coordinates with the CPET mechanism along the diagonal. Any transition state that falls within the step-wise borders but not along the diagonal is considered imbalanced with ET-like above the diagonal and PT-like below.

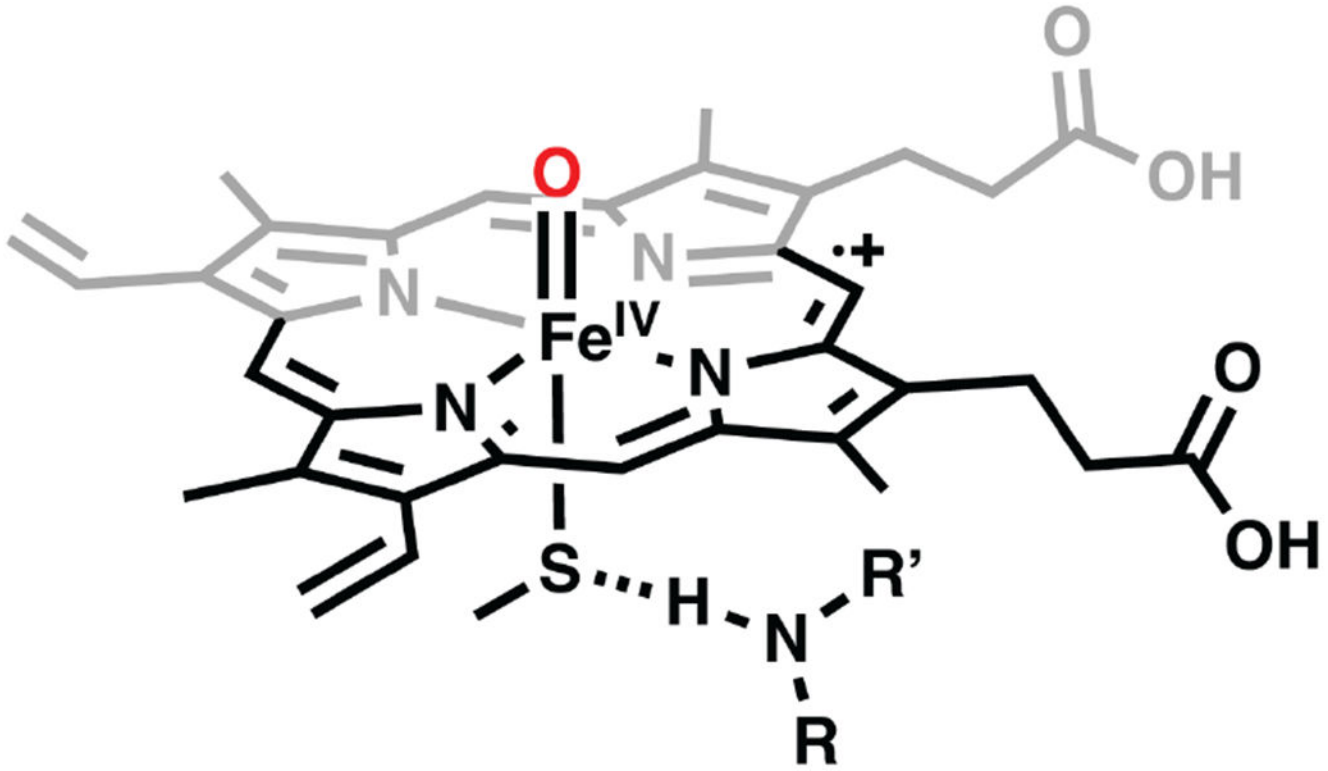

Figure 3.
H-bond to axial thiolate of compound I intermediate of P450.

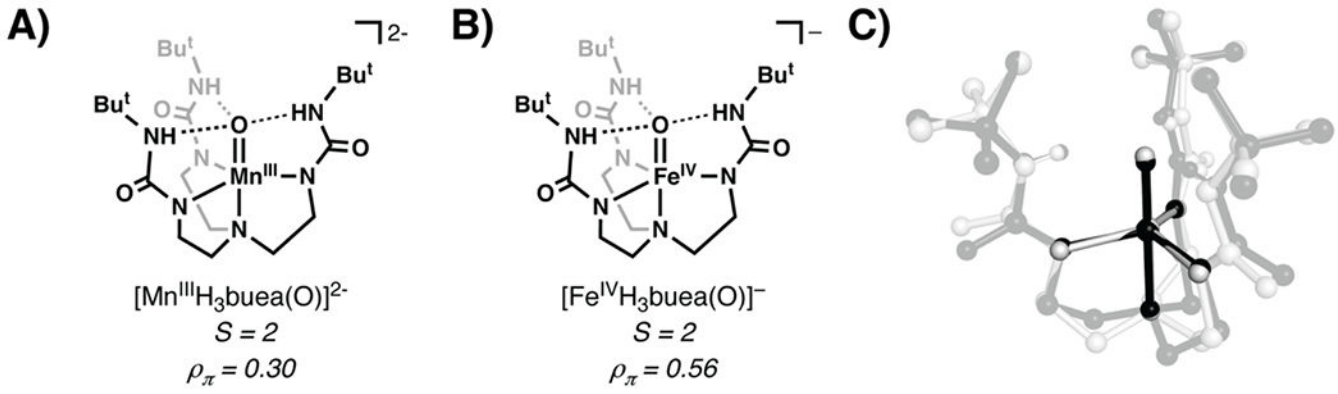

Figure 4.

Structures, spin ground states (*S*), and oxido spin densities ($\rho\pi$) experimentally derived of (A) $[Mn^{III}H_3buea(O)]^-$ and (B) $[Fe^{IV}H_3buea(O)]^-$. (C) Overlay of the molecular structures of $[Mn^{III}H_3buea(O)]^{2-}$ (gray) and $[Fe^{IV}H_3buea(O)]^-$ (black).

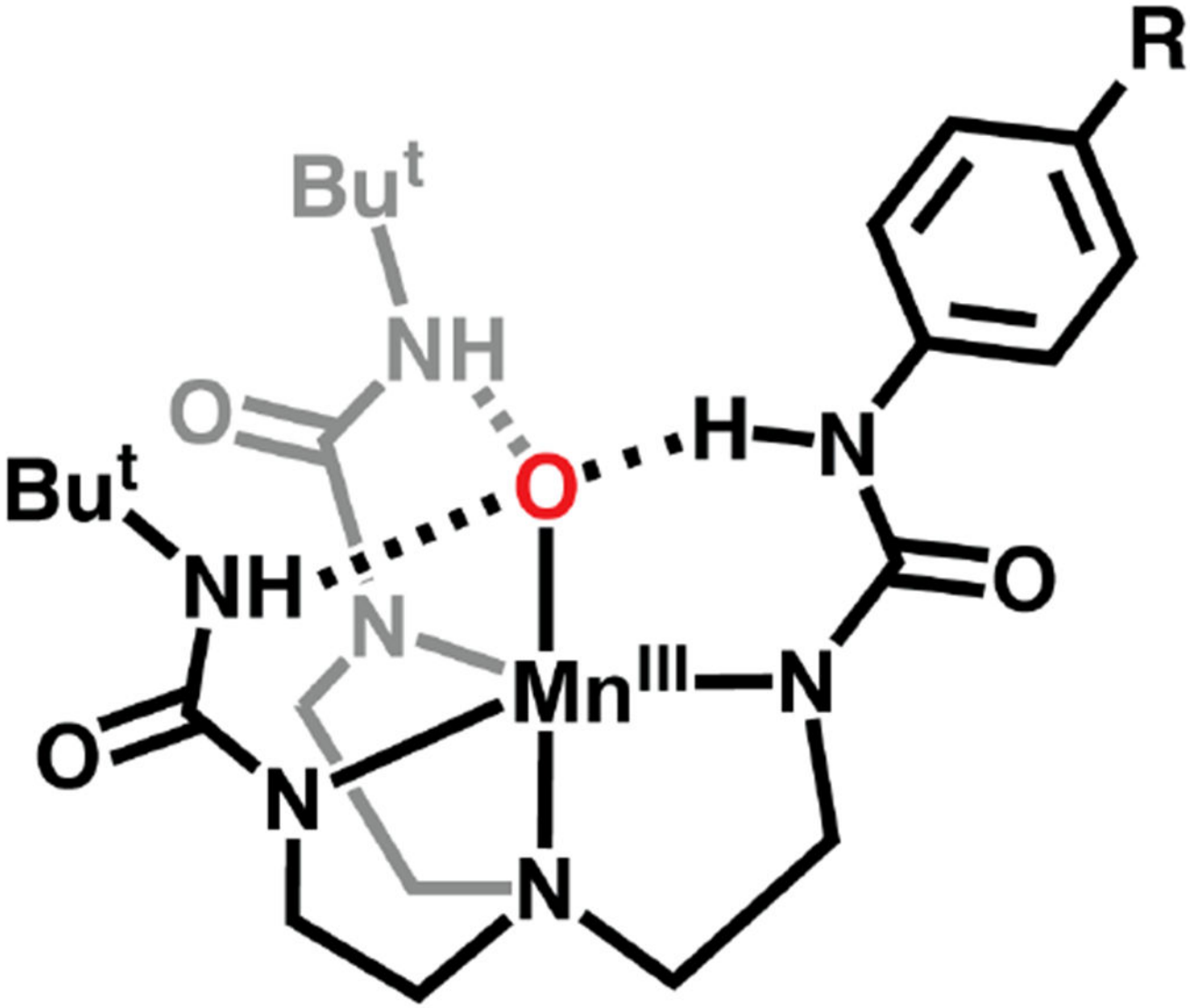

Figure 5.

Intramolecular H-bonding network involving a reactive Mn^{III}–oxido unit within a series of synthetic Mn^{III} complexes, $[Mn^{III}H_3bpuea\text{-}R(O)]^{2-}$ (R = OMe, H, Cl, F, CF_3).

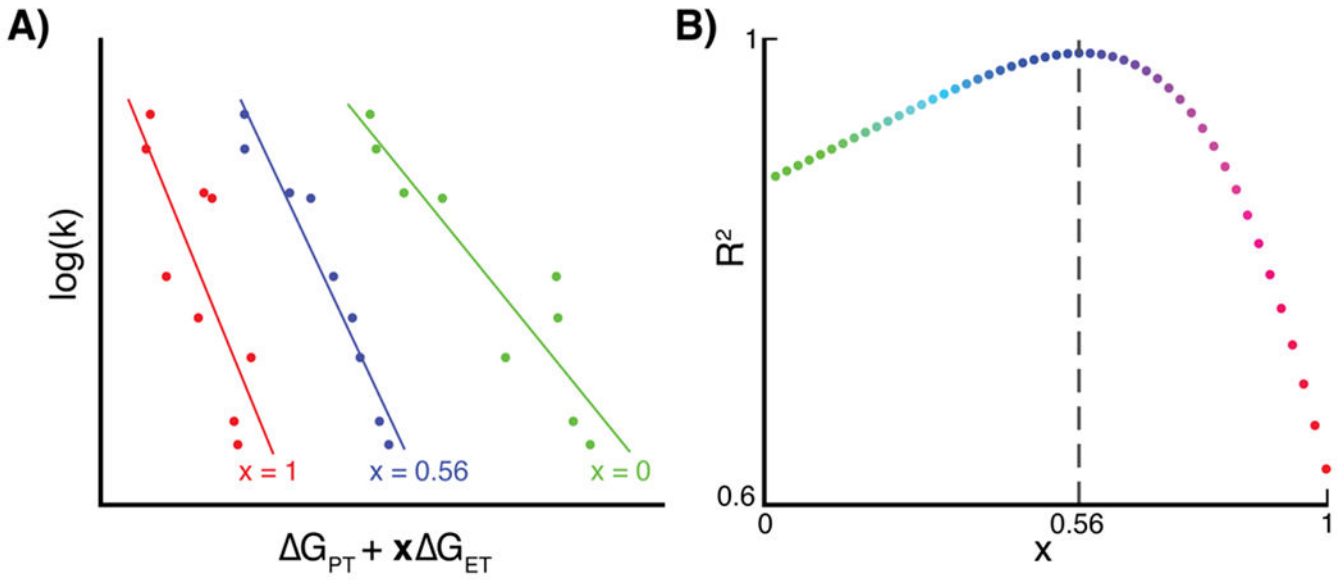

Figure 6.

Semi-empirical analysis of our Mn^{III} complex, $[Mn^{III}H_3bpuea\text{-}R(O)]^{2-}$, reacting with various substrates. (A) Plot of log (k) versus $\Delta G^{\circ}_{PT} + x \Delta G^{\circ}_{ET}$ highlighting fits of our reaction data to PT-driven (x = 0) (green), equally PT-and ET-driven (x=1) (red), and PT-dominated or imbalanced mechanisms. (B) Plot of R^2 of the lines of best fit versus x demonstrating that when x=0.56, R^2 is maximized.

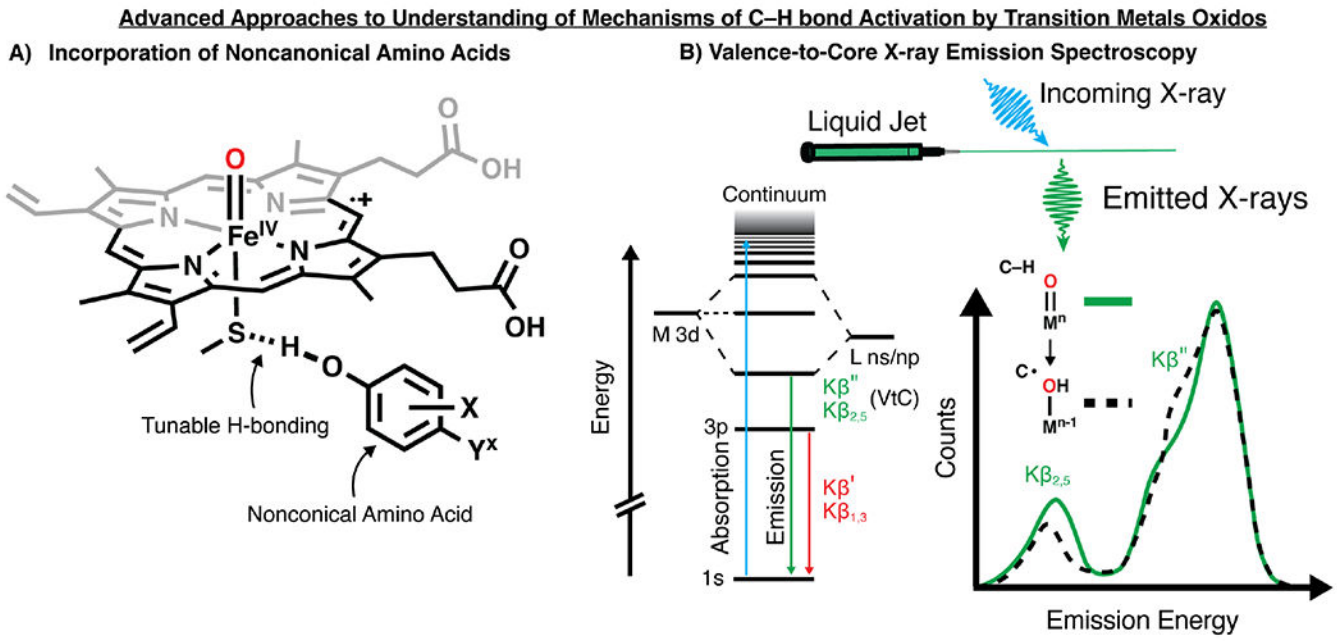

Figure 7.

Frontier approaches for studying mechanisms and the role of basicity in the activation of C–H bonds by transition metal oxido complexes. (A) Modulation of hydrogen bond strength to metallocofactors with noncanonical amino acid incorporation to tune thermodynamic properties through secondary coordination sphere effects. (B) X-ray emission spectroscopy as a sensitive probe of metal-ligand protonation state. X-rays are absorbed by the sample (blue) and then emitted at lower energies (green and red) upon electronic relaxation. Illustrative spectra demonstrate potential expected differences in the emission spectral profiles that can be used to differentiate between oxido ligand protonation states upon examination of the valence-to-core K-edge energies and intensities.